ISSN 0208-7774 TRIBOLOGIA 3/2020 p. 63–76
DOI: 10.5604/01.3001.0014.4766

Krzysztof WIERZCHOLSKI[*], Ryszard MACIOŁEK[**]

A NEW CONTRIBUTION IN STOCHASTIC HYDRODYNAMIC LUBRICATION FOR ARBITRARY BIO-SURFACES

NOWY WKŁAD DO LOSOWEGO HYDRODYNAMICZNEGO SMAROWANIA DOWOLNYCH POWIERZCHNI BIOLOGICZNYCH

Key words: movable non-rotational curvilinear bio-surfaces, hydrodynamic stochastic lubrication, non-Newtonian bio-fluid, phospholipids bilayer, viscosity depended on the gap height random variations, estimation of semi analytical solutions.

Abstract: This paper shows a recent progress described in curvilinear, orthogonal coordinates of the method of estimation of stochastic bio-hydrodynamic lubrication parameters. Here are discussed real arbitrary movable, non-rotational living biological surfaces coated with phospholipid bi-layers and lubricated with biological liquids. Non-rotational, curvilinear cooperating biological surfaces take the place in various biological nods for example in sacra bone, femoral bone, knee cap, calf bone and hip joint, elbow joint, knee joint, jump joint. Moreover are assumed biological non-rotational friction nods between human skin and tightly sport dress lubricated with the sweat. The main focus of the paper was to demonstrate the influence of expected values variations and standard deviation of the human joint gap height on the hydrodynamic lubrication parameters occurring during the friction process. It is very important to notice that the random gap height variations imply on the apparent dynamic viscosity of biological fluid or synovial fluid.

Słowa kluczowe: ruchome, nieobrotowe, krzywoliniowe powierzchnie biologiczne, losowe smarowanie, zmiana lepkości po grubości warstwy, dwuwarstwa fosfolipidów, oszacowania wartości semi-analitycznych rozwiązań.

Streszczenie: Niniejsza praca ujmuje nowe osiągnięcia autorów w zakresie metod oszacowywania losowych wartości hydrodynamicznych parametrów smarowania dla biologicznych powierzchni opisanych w krzywoliniowych ortogonalnych współrzędnych. Badania dotyczą dowolnych, ruchomych nieobrotowych, żywych powierzchni biologicznych pokrytych dwuwarstwą fosfolipidów, smarowanych cieczą biologiczną, fizjologiczną. Omawiane powierzchnie smarowane cieczą synowialną występują w węzłach tarcia biologicznego w stawach człowieka takich jak biodro, kolano, łokieć, paliczki, skok oraz między innymi na kości obojczykowej, łopatkowej, promieniowej, piszczelowej. Ponadto smarowanie potem występuje w węźle tarcia pomiędzy skórą człowieka a obcisłym dresem sportowym. Główne wysiłki autorów koncentrują się na badaniu wpływu zmian wartości oczekiwanej oraz odchylenia standardowego wysokości szczeliny smarnej na parametry tarcia i smarowania w węzłach tarcia biologicznego. Należy wyraźnie podkreślić, że losowe zmiany wysokości szczeliny mają wpływ na zmiany lepkości biologicznego czynnika smarującego.

INTRODUCTION

The topic of the presented paper concerns the probabilistic method of solutions of the lubrication of two movable but non-rotational, curvilinear living biological surfaces. The superficial layer of living bio-surfaces and the overlaying phospholipid bilayer membrane, only several nanometres thick, shape the height (several micrometre thick) of the considered gap between two cooperating bio-surfaces **[L. 1–4]**. The surface coated with phospholipids (PLs) and total gap height ε_T between cooperating surfaces are generally subject to several stochastic changes in relation to the nominal mean value. Random changes can be caused by micro vibrations, discrete load cumulated on the friction node, changes in roughness geometry of cooperating

[*] ORCID: 0000-0002-9074-4200. University of Economy (WSG). Garbary 2 Street, 85-229 Bydgoszcz, Poland, e-mail: krzysztof.wierzcholski@wp.pl.
[**] ORCID: 0000-0002-1507-9677. University of Economy (WSG). Garbary 2 Street, 85-229 Bydgoszcz, Poland, e-mail: maciolek@byd.pl.

surfaces, or genetic and volumetric growth of live cells on the living surface with a phospholipid layer **[L. 5–7]**.

The numerous previous experimental studies on the scope of the influence of the phospholipid membrane on the hydrodynamic process of surface lubrication were mainly focused on theory and experiments only for human rotational joints in the field of chemistry, without taking into account random changes **[L. 8–18]**. There has been no previous stochastic research concerning frictional forces and coefficients of friction based on experimental methods and analytical-numerical hydrodynamics for lamellar and laminar liquid flows between two non-rotational biological surfaces **[L. 12**, **17]**. Random gap height changes between two cooperating surfaces have a direct and indirect influence on lubrication parameters such as pressure, capacity, and friction forces. The direct influence is demonstrated by integral formulas determining lubrication parameters. The indirect influence of random changes in the articular bio-surface region coated with PLs on the value of lubrication parameters takes place through random changes in the dynamic viscosity of bio-fluid, which randomly affects changes in friction forces and pressure. In order to explain this phenomenon, it is necessary to consider the fact that apparent viscosity η_T of bio-fluid in the gap increases (decreases) together with increasing (decreasing) surface coated with PLs **[L. 19–22]**. Viscosity changes not only in the direction of the length and width of the flow, significant changes in viscosity are also revealed in the direction of the nanometre thickness of the layer. The aim of the research undertaken in this work is the following:

1. To directly and indirectly explain the influence of the randomly changing gap height between two cooperating non-rotational, curvilinear bio-surfaces on the values of hydrodynamic pressure and friction forces.
2. To show an estimation of the expected values of the main bio-tribology parameters based on the performed numerical solutions of random hydrodynamic equations for non-rotational bio-surfaces and measurements.

In the ankle joint, collar, or shoulder blade bone node, we can find the lubrication regions between two non-rotational not parallel or seldom parallel cooperating surfaces **Figs. 1a, b,** and **2c**. A new phenomenon of hydrodynamic perspiration lubrication in random form is observed in non-rotational, non-parallel curvilinear or exceptionally in non-rotational parallel movable surfaces, e.g., human skin surface and the tightly fitting clothing surface during gymnastic training **Figs. 1c, 2d** Half-rotational, curvilinear cooperating living surfaces are occurring in the human wrist joint and knee joint **Figs. 1a, b,** and **2b**. Rotational cooperating biological bone surfaces are also found in hip joints and elbow joints **Figs. 1a, b,** and **2a.**

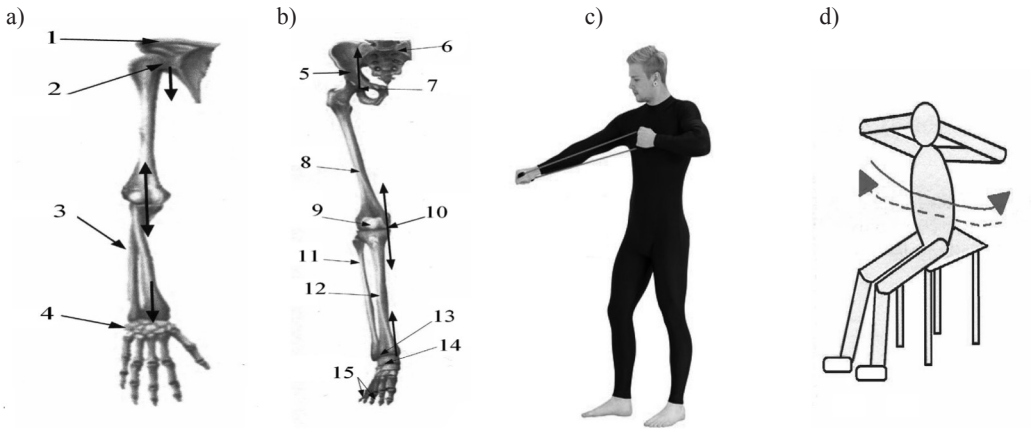

Fig. 1. Biological human friction nodes lubrication: a) upper human limb: 1 – collar bone, 2 – shoulder blade bone, 3 – radial bone, 4 – wrist joint; b) lower human limb: 5 – hip bone,6 – sacra bone, 7 – hip joint, 8 – femoral bone, 9 – knee cap, 10 – knee joint, 11 – calf bone, 12 – tibia, 13 – synsdesmosis, 14 – ankle joint, 15 – phalangeal joint; c) friction node between skin and tightly clothing

Rys. 1. Smarowanie biologicznych węzłów tarcia człowieka: a) kończyna górna:1 – kość obojczykowa, 2 – kość łopatkowa, 3 – kość promieniowa, 4 – kość nadgarstkowa; b) kończyna dolna: 5 – kość biodrowa, 6 – kość krzyżowa, 7 – staw biodrowy, 8 – kość udowa, 9 – rzepka, 10 – staw kolanowy, 11 – kość strzałkowa, 12 – kość piszczelowa, 13 – kość stępów, 14 – staw skokowy, 15 – stawy paliczkowe; c) węzeł tarcia pomiędzy skórą człowieka a obcisłym dresem sportowym

The variety of curvature shapes of the analysed non-rotational, cooperating bio-surfaces in human joint surfaces dictates the description of the surface in a curvilinear orthogonal coordinate system: α_1, α_2, α_3, where α_1 – width direction of the non-rotational surfaces or circumferential direction of the rotational surface, α_3 – longitudinal direction, α_2 – gap height direction. The joint gap is filled with physiological bio- fluid. We

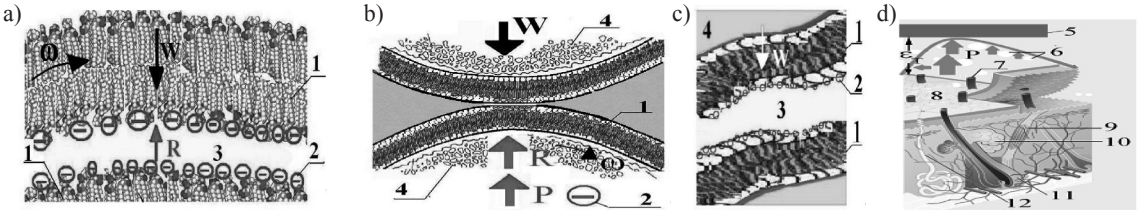

Fig. 2. Random gap height ε_T between two cooperating curvilinear biological surfaces: a) rotational, b) half – rotational, c) movable, non – rotational, d) movable, non – rotational (skin – persperation – clothing); 1 – phospholipid bilayer, 2 – hydrated phospholipid, 3 – biological liquid, 4 – subchondral bone, 5 – clothing, 6 – persperation, 7 – opening of persperation duct, 8 – human skin, 9 – muscle, 10 – gland, 11 – hair follicle, 12 – persperation duct; W – load, R – repulsion force, P – hydrodynamic pressure, ω – angular velocity

Rys. 2. Losowa wysokość szczeliny ε_T między współpracującymi biologicznymi powierzchniami: a) obrotowymi, b) półobrotowymi, c) ruchomymi nieobrotowymi, d) nieobrotowymi (skóra – pot – obcisły dres); 1 – dwuwarstwa fosfolipidów, 2 – nawodniona komórka fosfolipidy z ujemnym ładunkiem, 3 – biociecz, 4 – podchrzęstna, kolagen, 5 – dres, 6 – pot, 7 – otwarte ujście potu, 8 – pot, 9 – mięsień, 10 – gruczoł, 11 – włos, 12 – przewód potu, W – obciążenie, R – siła odpychająca, P – ciśnienie hydrodynamiczne, ω – prędkość kątowa

assume a characteristic constant dimensional gap height value ε_0 and dimensionless gap height function ε_{T1}, which is dependent on variables α_1 and α_3. This function is the sum of two parts described by the following formula (1) **[L. 23]**:

$$\varepsilon_{T1} = \varepsilon_T/\varepsilon_0 = \varepsilon_{T1s}(\alpha_1,\alpha_3)[1+\delta_1(\alpha_1,\alpha_3)]. \quad (1)$$

The symbol ε_{T1s} [m] denotes the dimensionless gap height limited by the nominally smooth biological non-rotational surfaces. Gap height ε_T has random changes caused by stochastic hyper-elastic deformations of articular superficial layer as well as random protrusions of the superficial layer or phospholipids bilayer surface roughness. The dimensionless random variable of corrections for gap height is marked with the symbol δ_1. The expected value for the random variable of corrections δ_1 is defined by the following formula (2) **[L. 24–25]**:

$$EX(\delta_1) \equiv \int_{-\infty}^{+\infty} (\delta_1) \times f(\delta_1) d\delta_1, \; EX(\delta_1)^2 \equiv \int_{-\infty}^{+\infty} (\delta_1)^2 \times f(\delta_1) d\delta_1, \; EX(\varepsilon_{T1}) = EX\left[\varepsilon_{T1s}\left(1+\delta_1\right)\right] = \varepsilon_{T1s}\left[1+EX(\delta_1)\right]. \quad (2)$$

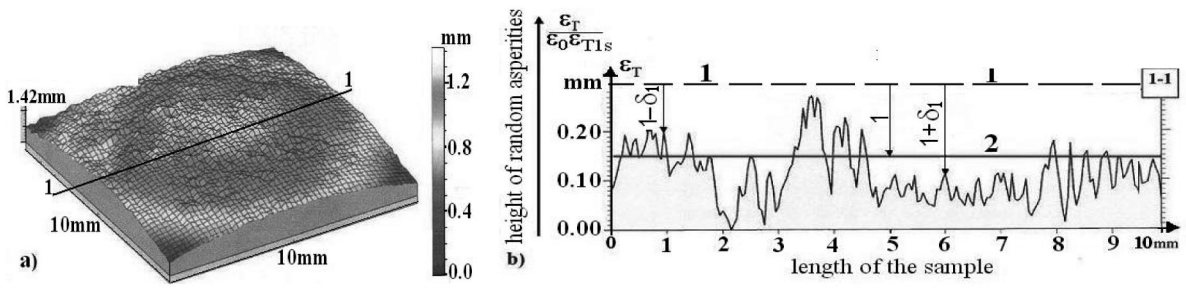

Fig. 3. Friction node surface structure and visualisation of random changes δ_1 in gap height ε_T caused by hyper-elastic deformations, unsteady load, and diseases, for the following: a) sample 10 mm×10 mm in an articular friction node; b) asperities along the cross section 1-1; 1 – central axis of the height of a gap with smooth surfaces, 2 – smooth surface limiting the gap without random changes

Rys. 3. Struktura powierzchni węzła tarcia oraz wizualizacja losowych zmian δ_1 wysokości szczeliny ε_T powodowanych przez hipersprężyste odkształcenia, zmienne obciążenia i schorzenia; a) próbka 10 mm × 10 mm, b) nierówności wzdłuż przekroju poprzecznego 1–1; 1 – oś środkowa wysokości szczeliny o gładkich powierzchniach, 2 – rzut gładkiej powierzchni ograniczający szczelinę bez zmian losowych

The symbol *EX* denotes the operator of the expected function. Probability density function *f* assigns probability values to the random variables of correction δ_1. The ordinates of density function *f* are probabilities established for the random corrections δ_1 of joint gap height. These values were determined experimentally and take into account articular superficial layer roughness. Standard deviation, σ, from the random

variable of corrections, is determined with the use of the following formula **[L. 24–25]**:

$$\sigma \equiv \sqrt{EX\left(\delta_1\right)^2 - EX^2\left(\delta_1\right)}. \tag{3}$$

Apart from gap height ε_T, phospholipid-coated surfaces, apparent dynamic viscosity η_T, hydrodynamic pressure, temperature, and other values are also subject to random change corrections. The surface structure of the tested samples is irregular due to the occurrence of random roughness (from 10 to 50 nm) or disease **[L. 26]**. Based on the comparisons made between the random changes in the rough superficial layer surface structure measured in Cwanek's research **[L. 1]** and Dowson's experiments **[L. 2]**, the probability density function is found to be unsymmetrical. The measurements of the random height changes in the surface roughness on cooperating non-rotational bio-surfaces were conducted using an articular friction sample (10mm×10mm) of the diseased superficial layer taken from a human shoulder blade bone **Figs. 3a, b**.The measurements were carried out using a laser micro-sensor installed in a Rank Taylor-Hobson-Taly-scan 150 apparatus. The results were compiled using Talymap-Expert and Microsoft Excel computer software. The measured gap height limited by the rough surfaces of the articular superficial layer of the presented sample varied from 0.05 to 0.25 mm **[L. 1]**.

SEMI-ANALYTICAL METHODS

Basic lubrication equations of two arbitrary surfaces in curvilinear coordinates

The lubrication problem of the non-rotational human nodes is presented by means of the conservation of momentum, continuity, Maxwell equations, the conservation of energy, and Young-Kelvin-Laplace's equation as well for biological non-Newtonian liquid, in particular, the case as a synovial or perspiration liquid lubrication flow. We assume a non-rotational, and unsteady, isothermal, incompressible flow of viscoelastic biological liquid in an electro-magnetic field. The abovementioned stochastic lubrication system of equations in curvilinear coordinates are expanded and written in the following curvilinear directions: α_1,α_2, and α_3.We take into account the expected functions (2) of unknown hydrodynamic pressure $EX[p(\alpha_1,\alpha_3)]$, unknown temperature $EX[T(\alpha_1,\alpha_2,\alpha_3)]$, the unknown velocity of bio-fluid $EX[v_i(\alpha_1,\alpha_2,\alpha_3)]$, viscosity of lubricating fluid $EX[\eta_T(\alpha_1,\alpha_2,\alpha_3)]$, and gap height $EX[\varepsilon_T(\alpha_1,\alpha_3)]$. The incompressibility of biological fluid enables one to ignore the influence of changes in the density of bio-fluid on changes in the equation for biological fluid flow continuity. We use the known dependences between interfacial energy γ and the power of hydrogen ion concentration *pH* and wettability *We* **[L. 18]**, **[L. 13–15]**. In basic equations, we take into account the influence of electrostatic field on the viscosity of bio-fluids studied by the authors **[L. 19, 23]** and the magnetic field is neglected.

We apply the classic boundary simplification of hydrodynamic equations in the boundary layer by omitting the terms of the order of relative radial clearance ψ with a value of 10^{-4}. Relative radial clearance ψ is defined as the ratio of the thickness of the thin bio-fluid layer ε_T to the length of the lubricated region of the non-rotational surface or curvature radius of the rotational surface flowed around.

After performing the transformations and calculations and applying the probabilistic changes (2, 3), and taking PLs into account **[L. 19–20]**, the mentioned system of equations for hydrodynamic lubrication of two arbitrary, non-rotational, biological cooperating surfaces in curvilinear coordinates has the following form **[L. 23]**:

$$0 = -\frac{1}{h_1}\frac{\partial EX\left(p\right)}{\partial \alpha_1} + \frac{\partial}{\partial \alpha_2}\left\{EX\left[\eta_T\left(\alpha_1,\alpha_2,\alpha_3\right)\right]\frac{\partial EX\left(v_1\right)}{\partial \alpha_2}\right\} + \rho_e E_1, \tag{4}$$

$$0 = \frac{\partial EX\left(p\right)}{\partial \alpha_2}, \tag{5}$$

$$-\frac{\rho EX\left(v_1^2\right)}{h_1 h_3}\frac{\partial h_1}{\partial \alpha_3} = -\frac{1}{h_3}\frac{\partial EX\left(p\right)}{\partial \alpha_3} + \frac{\partial}{\partial \alpha_2}\left\{EX\left[\eta_T\left(\alpha_1,\alpha_2,\alpha_3\right)\right]\frac{\partial EXv_3}{\partial \alpha_2}\right\} + \rho_e E_3, \tag{6}$$

$$\frac{1}{h_1 h_3}\frac{\partial}{\partial \alpha_1}\left[h_3 EX\left(v_1\right)\right] + \frac{\partial}{\partial \alpha_2}\left[EX\left(v_2\right)\right] + \frac{1}{h_1 h_3}\frac{\partial}{\partial \alpha_3}\left[h_1 EX\left(v_3\right)\right] = 0, \tag{7}$$

$$\frac{\partial}{\partial \alpha_2}\left\{\kappa\frac{\partial EX\left[T\left(\alpha_1,\alpha_2,\alpha_3\right)\right]}{\partial\, \alpha_2}\right\} + EX\left[\eta_T\left(\alpha_1,\alpha_2,\alpha_3\right)\right]\left\{\left[\frac{\partial EX\left(v_1\right)}{\partial \alpha_2}\right]^2 + \left[\frac{\partial EX\left(v_3\right)}{\partial \alpha_2}\right]^2\right\} = \frac{\boldsymbol{J}^2}{\sigma_e}, \tag{8}$$

where from Young-Kelvin-Laplace's equation follows that the expected function of apparent viscosity η_T[Pas] **[L. 19–20**, **23–24]** is:

$$EX\eta_T(\alpha_1,\alpha_2,\alpha_3) = EX\eta_T(n, p_H, We, T, \gamma, E) \equiv$$

$$= \frac{\gamma_{\max}(\mathrm{p}_H, \mathrm{We}) + kEX\left(A^{-1}\right)\cdot EX(T)\ln L}{\delta_v \cdot EX(v_0)}\left[1+\delta_E(p_H,E)E^2\right]\left(\sqrt{\left(\frac{\partial EXv_1}{\partial\alpha_{21}}\right)^2+\left(\frac{\partial EXv_3}{\partial\alpha_{21}}\right)^2}\right)^{n-1}, \quad (9)$$

for: $0 < L < 1{,}0 \le h_1\alpha_1 \le 2a$, $-b \le h_3\alpha_3 \le b$, $0 \le \alpha_2 \le EX(\varepsilon_T)$.Symbol 2a[m],2*b*[m] denote width and length of the friction region of two cooperating surfaces. We denote the following: *E*[V/m] – electric intensity vector, *J* [A/m^2] − electric current density, *v* [m/s] – biological fluid velocity, σ_e [S/m] − electrical conductivity of phospholipids bilayer, κ [/mK] – thermal conductivity coefficient for biological fluid, *T*[K] – temperature, ρ_e [C/m^3 = As/m^3] − electric space charge in biological fluid, γ [mJ/m^2 = N/m] − interfacial energy, $\gamma_{\max}$ − is the maximum interfacial energy of the lipid membrane whereas 0.1mN/m < γ_{max} < 4mN/m, *A* [m^2] − the region of areas of different phospholipids (PL) molecules concentration, i.e. of different superficial layer susceptibility, ρ [kg/m^3] − biological fluid density. Due to the presence of the phospholipids bi-layers on the cartilage or superficial layer surface and the presence of liposomes, micelles, macromolecules, and lamellar aggregates in biological fluid, this liquid has non-Newtonian, especially pseudo-plastic properties.

Symbol $k = 1.38054 \cdot 10^{-23}$ [J/K] – denotes Boltzmann constant. It follows from Formula (9) that apparent viscosity η_T [Pas] of biological liquid in the gap increases (decreases) together with increasing (decreasing) boundary surfaces for $10^{-16}\mathrm{m}^2 < A < 10^{-4}\mathrm{m}^2$. Dimensionless symbol δ_v occurring in formula (9) denotes dimensionless random coefficient ($0.2 < \delta_v < 0.6$). The bio-fluid dynamic viscosity decreases when index δ_v increases from 0.2 to 0.6. Coefficient δ_v describes the concentration c_c of collagen fibres in the bio-fluid. For $\delta_v = 0.2$ we have $c_c = 100\ 000$ mol/mm^3, while for $\delta_v = 0.6$ concentration equals $c_c = 100$ mol/mm^3. Since $0 < L < 1$, thus *lnL* is a negative number, while it is always the case that $\gamma_{max} > -kA^{-1}T\ lnL$, where $-100 < lnL < -10$.The symbol 0.03 m/s < v_0 < 0.04 m/s denotes the characteristic dimensional value of linear velocity for the bio-surface being flowed around. The derivatives in dimensionless gap height direction α_{21} of the terms described by dimensionless functions v_{11}, v_{31} of velocity vector components v_1 [m/s], v_3 [m/s] in directions α_1, α_3 in Formula (9) is a result of dimensionless transformations, where $v_1 = v_0 v_{11}$, $v_3 = v_0 \mathrm{I}_1$. The symbol *n* denotes dimensionless flow index ($0.8 < n < 1.2$), where, for $n = 1$, we have a Newtonian fluid. The following was assumed: δ_E [m^2/V^2] – experimental coefficient of the influence of electrical intensity *E* and concentration of hydrogen ions *pH* in the bio-fluid on the dynamic viscosity of the bio-fluid. The value of coefficient δ_E[m^2/V^2] for the bio-fluid has not yet been accurately measured experimentally. We only know that for $E = 10$ V/m and $pH = 8$, we obtain $\delta_E = 0.0003$ m^2/V^2 **[L. 27]**. It thus follows that the dimensionless increase in the dynamic viscosity of the bio-fluid resulting from the influence of electrostatic field in the phospholipid layer is $1+\delta_E E^2 = 1.03$, i.e. only 3%. Based on the estimations obtained, we can see that the direct influence of electrostatic field in the tissue boundary layer is negligible. Formula (9) was derived from known dependences of interfacial energy $\gamma(pH,We)$ describing the relationship between power of hydrogen ion concentration *pH* and wettability *We*. Interfacial energy was analytically transformed into the apparent dynamic viscosity of the lubricating fluid η_T. Such dependences are illustrated graphically in the work of **[L. 19]** for two types of phospholipids, PC and PS. Viscosity increases in interval $2 < pH < 4$ and decreases in interval $4 < pH < 10$. Bio-fluid dynamic viscosity for PC and PS lipids increases with increasing power of hydrogen ion concentration *pH* to certain isoelectric point IP ($\gamma = 3.5$ mJ/m^2) with established values *We,* δ_v, *T,* and v_0. A further increase in *pH* causes a decrease in dynamic viscosity. The dynamic viscosity of the bio-fluid decreases with decreasing wettability *We* at established values δ_v, *T,* and v_0. Drops in wettability from 70° to 50° indicate a transition from the hydrophobic to hydrophilic properties of the bio-surfaces flowed around by the bio fluid.

For two arbitrary cooperating biological surfaces, we apply the curvilinear, orthogonal system of co-ordinates α_1, α_2, and α_3 with the respective Lamé coefficients h_1, h_2, and h_3. After the abovementioned boundary simplifications of the thin arbitrary, curvilinear, non-rotational non-parallel surfaces, it follows that $h_2 = 1$ and $h_1 = h_1(\alpha_1, \alpha_3)$, $h_3 = h_3(\alpha_1, \alpha_3)$. For example, this case is valid for the ankle joint, collar bone, and shoulder blade. Moreover, this is also the case for the thin perspiration layer between the non-rotational movable external skin surface and the surface of tightly fitting clothing. For the thin liquid layer restricted by the two rotational surfaces in the α_1 direction and non-monotone generating line in the α_3 direction, the Lame coefficients are as follows: $h_2 = 1$, $h_1 = h_1(\alpha_3)$, $h_3 = h_3(\alpha_3)$ or $h_3 = 1$ for monotone generating line. This case is valid for human elbow joints, and hip joints.

Similarly to Formulas (1) and (2), specifying random gap height changes, expected functions of pressure, temperature, and lubricating fluid velocity components, occurring in the system of Equations (4) to (8), take the following forms **[L. 23]**:

$$EX(p) = p(\alpha_1,\alpha_3)[1+EX(\delta_p)],\ EX(T) = T(\alpha_1,\alpha_2,\alpha_3)[1+EX(\delta_T)],\ EX(v_i) = v_i(\alpha_1,\alpha_2,\alpha_3)[1+EX(\delta_{vi})] \quad \text{for } i = 1, 2, 3, \quad (10)$$

where the symbols δ_p, δ_T, and δ_{vi} denote unknown random variables of pressure, temperature, and biological fluid velocity component corrections. If the random variable of gap height corrections $\delta_1 = 0$, then also $\delta_p = \delta_T = \delta_{vi} = 0$. In this case, $EX(\delta_p) = EX(\delta_T) = EX(\delta_{vi}) = 0$; therefore, under assumption (10), we have: $EX(p) = p$, $EX(T) = T$, $EX(v_i) = v_i$ for $i = 1, 2, 3$. Thus, in this special case, the system of Equations (4) – (8) loses stochastic properties.

The system of partial differential Equations (4) – (8) determines the following expected functions of randomly variables unknowns, namely, three bio-fluid velocity vector components $EX[v_i(\alpha_1, \alpha_2, \alpha_3)]$ [m/s] for $i = 1, 2, 3$; hydrodynamic pressure $EX[p\ (\alpha_1, \alpha_3)]$ [Pa], and temperature $EX[T(\alpha_1, \alpha_2, \alpha_3)]$ [K]. The term on the left side of Equation (6) describes the centrifugal forces occurring during the cooperation of two bio-surfaces. These forces occur only when Lamé coefficient h_1 is a function of α_3. This applies to the non-rotational, curvilinear bio-surface or only to rotational bio-surfaces resting on a bone head with a non-monotone generating line, e.g., for spherical, conical, parabolic, or elliptical shapes, but not cylindrical shapes, where coefficient h_1 is a constant value.

Integrals for random hydrodynamic lubrication of non-rotational surfaces

The integration of the system of Equations (4) – (8) describing the lubrication of two non-rotational bio-surfaces with the participation of phospholipids (PL) separated by a thin layer of biological fluid with viscosity variations in gap height direction will be carried out in curvilinear coordinates (α_1, α_2, α_3). The lubricated bio-surface performs a non-rotational motion with linear velocity $U_1(\alpha_1, \alpha_3)$ [m/s] in the α_1 direction and $U_3(\alpha_1, \alpha_3)$ [m/s] in the α_3 direction, while the second bio-surface is stationary and limits a gap filled with a layer of bio-fluid of randomly varying height ε_T. The randomly varying expected pressure $EX(p)$ is determined from Equations (4) to (7), assuming the value of atmospheric pressure p_A at the edges of lubrication area $\Omega(\alpha_1, \alpha_3)$ defined by the topological boundary operator Fr. Therefore, we apply the following boundary conditions to the function components of expected randomly varying bio-fluid velocities $EX(v_1)$, $EX(v_2)$, and $EX(v_3)$ in α_1, α_2, and α_3 and pressure $EX(p)$ in the α_1 and α_3 directions **[L. 23]**:

$$EX(v_1) = U_1 \quad \text{for } \alpha_2 = 0,\ EX(v_1) = 0 \text{ for } \alpha_2 = EX(\varepsilon_T), \quad (11)$$

$$EX(v_2) = 0 \quad \text{for } \alpha_2 = 0, \text{ and } EX(v_2) = 0 \text{ for } \alpha_2 = EX(\varepsilon_T), \quad (12)$$

$$EX(v_3) = U_3 \text{ for } \alpha_2 = 0,\ EX(v_3) = 0 \text{ for } \alpha_2 = EX(\varepsilon_T). \quad (13)$$

$$EX[p(\alpha_1,\alpha_3)] = p_A \text{ for } (\alpha_1,\alpha_3) \in Fr\Omega,\ \Omega \in (0 \le h_1\alpha_1 \le a)\times(-b \le h_3\alpha_3 \le b). \quad (14)$$

In order to determine expected function of randomly variable temperature $EX[T(\alpha_1, \alpha_2, \alpha_3)]$ from second order differential Equation (8), two boundary conditions are required. The decreases and increases in the expected function of temperature below and above characteristic temperature T_0 ultimately give constant temperature value f_c on the first bio-surface (movable) and the variable unknown value of temperature changes $f_p(\alpha_1,\alpha_3)$ on the second bio-surface (immovable). Thus, the two searched boundary conditions are as follows **[L. 23]**:

$$EX[T(\alpha_1, \alpha_2, \alpha_3)] = T_0 + f_c \text{ for } \alpha_2 = 0, \quad (15a)$$

$$EX[T(\alpha_1, \alpha_2, \alpha_3)] = T_0 + f_p(\alpha_1, \alpha_3) \text{ for } \alpha_2 = EX(\varepsilon_T). \quad (15b)$$

By applying these conditions (11-13) to the general solution of Equations (4) to (7), for i = 1,3, we obtain the following form of the function of the expected randomly variable component of bio-fluid velocity vector in directions α_1, α_2, and α_3, for the non-rotational movable bio-surface **[L. 21]**:

$$EX\left[v_i\left(\alpha_1,\alpha_2,\alpha_3\right)\right] = EX\left[\Pi_i\left(\alpha_1,\alpha_3\right)\right]A_\eta + (1-A_s)U_i - \delta_{i3}\frac{\rho}{h_1h_3}\frac{\partial h_l}{\partial\alpha_3}A_p, \quad i = 1, 3, \quad (16a)$$

$$EX\left[v_2\left(\alpha_1,\alpha_2,\alpha_3\right)\right] = -\int_0^{\alpha_2}\frac{1}{h_1h_3}\frac{\partial\left(h_3v_1\right)}{\partial\alpha_1}d\alpha_2 - \int_0^{\alpha_2}\frac{1}{h_1h_3}\frac{\partial\left(h_1v_3\right)}{\partial\alpha_3}d\alpha_2 .\ EX\left[\Pi_i\left(\alpha_1,\alpha_3\right)\right] \equiv \frac{1}{h_i}\frac{\partial EX(p)}{\partial\alpha_i} - M_i, \quad (16b)$$

where $\delta_{ij} = 1$ *for* $i = j$ and $\delta_{ij} = 0$ *for* $i \neq j$; $M_i = \rho_e E_i$[N/m^3]; $0 \le h_1\alpha_1 \le 2a$[m]; $-bh_3\alpha_3 \le b$[m]; $h_1\alpha_1$[m]; $h_3\alpha_3$[m]; α_2[m].

For thin, arbitrary, cooperating biological non-rotational surfaces in the α_1 and α_3, directions, where $h_2 = 1$, $h_1 = h_1(\alpha_1,\alpha_3)$, and $h_3 = h_3(\alpha_1,\alpha_3)$, for a movable surface in the α_1 direction with linear velocity U_1 and in the α_3 direction with linear velocity U_3, and for surfaces lubricated with the liquid where dynamic viscosity varies in three directions: η_T (α_1, α_2, α_3), then, we obtain the following stochastically modified Reynolds equations determining expected function $EX[p(\alpha_1, \alpha_3)]$ of randomly variable hydrodynamic pressure **[L. 23]**:

$$\begin{aligned}&\frac{1}{h_1h_3}\frac{\partial}{\partial\alpha_1}\left[h_3\left(\frac{\partial EX(p)}{h_1\partial\alpha_1}-M_1\right)\left(\int_0^{EX(\varepsilon_T)}A_\eta d\alpha_2\right)\right]+\frac{1}{h_1h_3}\frac{\partial}{\partial\alpha_3}\left[h_1\left(\frac{\partial EX(p)}{h_3\partial\alpha_3}-M_3\right)\left(\int_0^{EX(\varepsilon_T)}A_\eta d\alpha_2\right)\right]+\\&-\rho\frac{1}{h_1h_3}\frac{\partial}{\partial\alpha_3}\left(\frac{\partial h_1}{h_3\partial\alpha_3}\int_0^{EX(\varepsilon_T)}A_p d\alpha_2\right)=\frac{1}{h_1h_3}\left\{\frac{\partial}{\partial\alpha_1}\left[U_1h_3\left(\int_0^{EX(\varepsilon_T)}A_s d\alpha_2-EX(\varepsilon_T)\right)\right]+\frac{\partial}{\partial\alpha_3}\left[U_3h_1\left(\int_0^{EX(\varepsilon_T)}A_s d\alpha_2-EX(\varepsilon_T)\right)\right]\right\},\end{aligned} \tag{17}$$

where $0 \le h_1\alpha_1 \le 2a$, $-b \le h_3\alpha_3 \le b$, $h_1\alpha_1$ [m], $h_3\alpha_3$ [m], α_2 [m], a[m], b[m], $U_i = U_i(\alpha_1, \alpha_3)$[m/s]; i = 1, 3. The terms multiplied by the linear velocity components U_1. U_3 are describing the influence of the non-rotational curvilinear surface motion on the hydrodynamic pressure value. Now we substitute the expected functions of bio-fluid velocity vector components (Equations 16a and b) to energy Equation (8). We take into account a constant value of bio-fluid thermal conductivity κ. For non-rotational arbitrary, cooperating biological surfaces in the α_1 and α_3 directions, where $h_2 = 1$ and $h_1 = h_1(\alpha_1,\alpha_3)$, $h_3 = h_3(\alpha_1,\alpha_3)$, we consider the linear velocity U_1 and U_3 in the α_1 and α_3 direction respectively and dynamic viscosity variations in three directions: η_T (α_1, α_2, α_3). Then after transformations and imposing boundary conditions (15), we obtain the expected function of temperature EX[$T(\alpha_1, \alpha_2, \alpha_3)$] in a randomly variable form. Subordinate functions A_s **[L. 1]**, A_η [m^4/Ns] occurring in Equations (16-17) are the following **[L. 23]**:

$$A_s(\alpha_1,\alpha_2,\alpha_3)\equiv\left(\int_0^{\alpha_2}\frac{1}{EX(\eta_T)}d\alpha_2\right)\left(\int_0^{EX(\varepsilon_T)}\frac{1}{EX(\eta_T)}d\alpha_2\right)^{-1},\ A_\eta(\alpha_1,\alpha_2,\alpha_3)\equiv\int_0^{\alpha_2}\frac{\alpha_2}{EX(\eta_T)}d\alpha_2-A_s(\alpha_1,\alpha_2,\alpha_3)\cdot\left(\int_0^{EX(\varepsilon_T)}\frac{\alpha_2}{EX(\eta_T)}d\alpha_2\right), \tag{18}$$

where $0 \le h_1\alpha_1 \le 2a$, $-b \le h_3\alpha_3 \le b$, $0 \le \alpha_2 \le EX(\varepsilon_T)$, $EX(\varepsilon_T) = EX[\varepsilon_T(\alpha_1, \alpha_3)]$, $h_1\alpha_1$ [m], $h_3\alpha_3$ [m], α_2 [m], a [m], b [m]. The term multiplied by the bio-fluid density ρ in Equation (16) and (17) describe the influence of the suction effect of the non-rotational bio-surface on the distribution of bio-fluid velocity, pressure, and temperature. The characteristic function of centrifugal effects A_p [m^6/Ns^3] was assumed as follows:

$$A_p(\alpha_1,\alpha_2,\alpha_3)\equiv EX\left[\Pi_1^2(\alpha_1,\alpha_3)\right]A_{\rho1}(\alpha_1,\alpha_2,\alpha_3)-2U_1EX\left[\Pi_1(\alpha_1,\alpha_3)\right]A_{\rho2}(\alpha_1,\alpha_2,\alpha_3)+U_1^2A_{\rho3}(\alpha_1,\alpha_2,\alpha_3), \tag{19}$$

where

$$A_{\rho i}(\alpha_1,\alpha_2,\alpha_3)\equiv\int_0^{\alpha_2}\left(\frac{1}{EX(\eta_T)}\int_0^{\alpha_2}\Gamma_{\rho i}d\alpha_2\right)d\alpha_2-A_s\int_0^{EX(\varepsilon_T)}\left(\frac{1}{EX(\eta_T)}\int_0^{\alpha_2}\Gamma_{\rho i}d\alpha_2\right)d\alpha_2,\ \Gamma_{\rho i}\equiv\left[\left(A_\eta\right)^{e_{i3}}\cdot\left(1-A_s\right)^{e_{i1}}\right]^{1+e_{i2}}. \tag{20}$$

Where $i = 1, 2, 3$; $e_{ij} = 1 - \delta_{ij}$; $0 \le h_1\alpha_1 \le 2a$, $-b \le h_3\alpha_3 \le b$, $0 \le \alpha_2 \le EX(\varepsilon_T)$, $EX(\varepsilon_T) = EX[\varepsilon_T(\alpha_1, \alpha_3)]$, $h_1\alpha_1$ [m], $h_3\alpha_3$ [m], α_2 [m], a[m], b[m], $U_1 = U_1(\alpha_1, \alpha_3)$[m/s]. The influence of centrifugal forces disappears when the Lame coefficient h_1 is independent of α_3. This situation occurs if we have two cooperating plates or rotational bio-surfaces, e.g., cylindrical cooperating surfaces where the generating line is a straight line parallel to the axis of rotation.

The components of expected random functions of friction forces F_{R1},F_{R3} [N] in curvilinear α_1 and α_3 directions, occurring during the lubrication of two non-rotational bio-surfaces with the participation of phospholipids (PL) separated by a thin layer of biological fluid with viscosity variations in gap height direction, η_T (α_1, α_2, α_3), will be formulated in curvilinear coordinates (α_1, α_2, α_3) in the following forms **[L. 23]**:

$$EX(F_{Ri})=\iint_\Omega\left[EX(\eta_T)\frac{\partial EX(v_i)}{\partial\alpha_2}\right]_{\alpha_2=EX(\varepsilon_T)}\cdot h_1h_3d\alpha_1d\alpha_3, \tag{21}$$

where i = 1, 3, $0 \le h_1\alpha_1 \le 2$a [m], $-b \le h_3\alpha_3 \le b$ [m], $h_1\alpha_1$ [m], $h_3\alpha_3$ [m], α_2 [m], a[m], b[m], $0 \le \alpha_2 \le EX(\varepsilon_T)$, $h_1 = h_1(\alpha_1, \alpha_3)$, $h_3 = h_3(\alpha_1, \alpha_3)$, $\Omega(\alpha_1, \alpha_3)$ – lubrication surface.

The expected value of load carrying capacity C [N] for non-rotational cooperating biological surfaces with h_2 = 1, $h_1 = h_1(\alpha_1, \alpha_3)$ and $h_3 = h_3(\alpha_1,\alpha_3)$ will be formulated in curvilinear coordinates in the following surface integral form:

$$EX(C) = \iint_{\Omega} EX\left[p(\alpha_1,\alpha_3)\right]\cdot d\Omega, \quad d\Omega = h_1h_3d\alpha_1d\alpha_3, \tag{22}$$

where $0 \le h_1\alpha_1 \le 2a$, $-b \le h_3\alpha_3 \le b$, $h_1\alpha_1$ [m], $h_3\alpha_3$ [m], α_2 [m], a[m], b[m]. Load carrying capacity is situated in vertical direction to the biological friction node surface Ω and in the opposite direction to load W[N].

Based on Coulomb's law of friction, taking into account expected function of adhesion force $EX(A_D)$ [N] in a curvilinear orthogonal coordinate system, the dimensionless, randomly variable coefficient of friction has the following form:

$$EX(\mu) = \frac{\left|e_1EX(F_{R1}) + e_3EX(F_{R3})\right| - EX(A_D)}{EX(C)}, \tag{23}$$

where e_1, e_3 are the unit vectors tangential to the α_1 and α_3 directions.

ESTIMATIONS AFTER NUMERICAL AND EXPERIMENTAL METHODS

Now we show general estimation of random lubricant parameters for the two non-rotational curvilinear cooperating biological surfaces. First, we are going to present an estimation of the value of the expected functions of random lubricant liquid velocity, random hydrodynamic pressure, load-carrying capacity, and friction forces for lubricated curvilinear arbitrary biological non-rotational surfaces, based on the stochastic gap height analysis (Section 2). By virtue of analytical solutions presented in Subsection 3.2, it follows that a non-rotational surface moves with linear velocity $U_i(\alpha_1,\alpha_3)$ [m/s] in the α_i direction for i = 1, 3, while the second bio-surface is stationary and limits a gap filled with a layer of bio-liquid of randomly varying height ε_T.

- Using probability density function f for corrections δ_1 of the gap height, obtained in experimental way, we determine the expected correction value, i.e. $EX(\delta_1) = m$, from Formula (2); and from Equation (3), we calculate standard deviation σ.
- For stationary flow of biological fluid in gap of the friction node between two surfaces, there is an equal volumetric flow rate in places of the narrowing and expansion of gap height ε_T, both in the case of classic hydrodynamic lubrication and by squeezing the lubrication out of the joint. The flow rate, as the product of average flow velocity and flow surface, implies an increase (decrease) in velocity v, which is inversely proportional to the narrowing (widening) of the gap height. Using the expected value of gap height corrections m, and its standard deviation σ and taking into account numerical estimations of analytical velocity solutions (16ab), we then have the following inequalities presenting the estimation for the value of the expected velocity function:

$$\frac{1}{1+m+\sigma} \le \frac{EX(v)}{v(\delta_1 = 0)} \le \frac{1}{1+m-\sigma}, \quad v(\delta_1 = 0) = O(U), \quad U \equiv \sqrt{U_1^2 + U_3^2}, \tag{24}$$

where $v(\delta_1 = 0)$ denotes the velocity without random corrections of gap height.

- The apparent viscosity changes are confirmed by the Kelvin-Laplace formula (Formula 9) defining apparent viscosity η_T. In this formula, an increase (decrease) in velocity v implies a decrease (increase) in the dynamic viscosity of biological fluid. Thus, using the expected value of gap height corrections m, and its standard deviation σ and after numerical estimations for expressions (Formula 9), we obtain the following inequalities presenting the estimation for the value of the expected viscosity function:

$$(1+m-\sigma) \le \frac{EX(\eta_T)}{\eta_T(\delta_1 = 0)} \le (1+m+\sigma), \qquad \eta_T(\delta_1 = 0) = O\left(\frac{\gamma_{max} + k\cdot A^{-1}T\cdot lnL}{\delta_v\cdot v_0}\right), \tag{25}$$

where $\eta_T(\delta_1 = 0)$ denotes the biological liquid viscosity without random corrections of gap height and without susceptibility random changes on the superficial layer of surfaces. By virtue of Equation (25), we calculate the apparent dynamic viscosity for SF taking into account the following parameter values: $A = 10^{-15}\,m^2$; $lnL = -50$; $\gamma = 2.5\ mJ/m^2$; 0.03 m/s < v_0 < 0.04 *m/s;* 0.2 < δ_v < 0.6; $T = 310\ K$; $k = 1.380649 \cdot 10^{-23}$. Hence, $kA^{-1}T \cdot lnL = -0.214$ mN/m.

The apparent viscosity of synovial fluid (SF) has the O(0.3105 Pas) value **[L. 23]**.

- The analytical and numerical solution of the system of Equations (4) to (8), which is Equation (17), shows that smaller gap height implies greater velocity and lower viscosity of non-Newtonian liquid. The expected function of hydrodynamic pressure $EX(p)$ estimated in numerical way from differential Equation (17), with the simultaneous use of results of Equations (24) and (25), enables one to obtain an estimation of the pressure in the following interval **[L. 23]**:

$$\frac{(1+m-\sigma)\cdot\alpha_p}{(1+m+\sigma)^2} \le \left(\frac{EX(p)}{p(\delta_1=0)} \equiv \xi_p\right) \le \frac{(1+m+\sigma)\cdot\beta_p}{(1+m-\sigma)^2}, \quad p(\delta_1=0) = O\left(\frac{U\cdot\eta_T(\delta_1=0)}{\psi\cdot\varepsilon_T(\delta_1=0)}\right), \quad \psi \equiv \frac{\varepsilon_T}{L_R}, \tag{26}$$

where $p(\delta_1 = 0)$ denotes the hydrodynamic pressure without random corrections of gap height, L_R – length of the lubrication region of the non-rotational surface. Correction coefficients α_p and β_p are dependent on radial clearance between two surfaces and on range of stochastic changes of dimensionless fraction ξ_p of pressure values.

- The expected values of load-carrying capacity $EX(C) = \Omega \cdot EX(p)$ for pressure $EX(p)$ and after numerical estimations obtained from Formula (22) for the lubricated surface $\Omega = d\alpha_1 d\alpha_3$ and for correction coefficients α_C, β_C are limited in the following interval:

$$\frac{(1+m-\sigma)\cdot\alpha_C}{(1+m+\sigma)^2} \le \left(\frac{EX(p)}{p(\delta_1=0)} \equiv \xi_p\right) \le \frac{(1+m+\sigma)\cdot\beta_C}{(1+m-\sigma)^2}, \quad C(\delta_1=0) = \Omega\cdot O\left(\frac{U\cdot\eta_T(\delta_1=0)}{\psi\cdot\varepsilon_T(\delta_1=0)}\right), \quad \Omega \equiv \iint_{\Omega} h_1 h_3 d\alpha_1 d\alpha_3, \tag{27}$$

where $C(\delta_1 = 0)$ denotes the load carrying capacity without random corrections of gap height.

- The expected function of friction forces $EX(F_R)$ with components estimated in numerical way from the formulas above (21), with the simultaneous use of inequalities, Equations (24), (25) and (26), enables us to show its upper and lower value presenting the friction force estimation in the following form:

$$\frac{(1+m-\sigma)\cdot\alpha_F}{1+m+\sigma} \le \left(\frac{EX(F_R)}{F_R(\delta_1=0)} \equiv \xi_F\right) \le \frac{(1+m+\sigma)\cdot\beta_F}{1+m-\sigma}, \quad F_R(\delta_1=0) = O\left(\frac{\Omega U\cdot\eta_T(\delta_1=0)}{\varepsilon_T(\delta_1=0)}\right), \tag{28}$$

where $F_R(\delta_1 = 0)$ is the friction force without random corrections of gap height, and α_F, β_F are the correction coefficients depending on the radial clearance of surfaces and on random changes of fraction ξ_F of friction values.

- The expected function of the coefficient of friction $EX(\mu)$, expressed by Formula (23), with the simultaneous use of inequalities, Formulas (27) and (28), neglecting the adhesion forces, and taking into account correction coefficients α_μ *and* β_μ, enables the estimation in the following interval:

$$(1+m-\sigma)\cdot\alpha_\mu \le \left(\frac{EX(\mu = F_R/C)}{\mu(\delta_1=0)} \equiv \xi_\mu\right) \le (1+m+\sigma)\cdot\beta_\mu, \quad \mu(\delta_1=0) = O\left(\frac{\varepsilon_T(\delta_1=0)}{L_R}\right), \tag{29}$$

where $\mu(\delta_1 = 0)$ denotes the friction coefficient without random corrections of gap height.

Now for some particular surfaces, we shall be considering the characteristic data for abovementioned estimations.

Example 1. We consider the human hip joint with two cooperating half spherical rotational surfaces. Lower surface (bone head) moves in the α_1 direction with angular velocity ω. The upper surface (acetabulum) is motionless. Both spherical surfaces are motionless in the meridian α_3 direction. Hence, we have $U_1 = h_1$, $U_3 = 0$ and $\alpha_1 = \varphi$, $\alpha_2 = r$, and $\alpha_3 = \vartheta$. Only part of the spherical surface region is lubricated with monotone generating line, i.e. inside the intervals: $0 < \varphi < \pi$; $\pi R/6 < \vartheta < \pi R/2, \vartheta = \vartheta_1 R$ – meridian coordinate. Thus, the

Lame coefficients are as follows: $h_1 = Rsin\vartheta_1$, $h_3 = 1$, $R[m] = L_R$ which denotes the radius of the sphere. Hence, $U, \Omega,$ and the gap height ε_T have the following form **[L. 23]**:

$$U \equiv \sqrt{U_1^2 + U_3^2} = \sqrt{(\omega R sin\vartheta_1)^2 + 0^2} = \omega R sin\vartheta_1, \quad \Omega \equiv \iint_{\Omega} h_1 h_3 d\alpha_1 d\alpha_3 = \frac{\sqrt{3}\pi R^2}{2}, \; \varepsilon_T(\phi, \vartheta_1, \delta_1) = \varepsilon_0 \varepsilon_{T1}(\phi, \vartheta_1, \delta_1). \tag{30}$$

We assume the centre of the spherical bone head to be at O (0.0.0). The centre of the spherical surface of the acetabulum is at $O_1(x - \Delta\varepsilon_x, y - \Delta\varepsilon_y, z + \varepsilon_z)$. Eccentricity has the value of D, see **Figs. 4a** to **e**.

Example 2. A geometrical simulation of the elbow cylindrical joint is presented in **Fig. 5a**. We consider the human elbow joint with two cooperating cylindrical rotational surfaces. Lower surface (bone head) moves in the α_1 direction with angular velocity ω. The upper surface (acetabulum) is motionless. Both cylindrical surfaces are motionless in length direction α_3. Hence, we have $U_1 = \omega h_1$, $U_3 = 0$ and $\alpha_1 = \varphi$, $\alpha_2 = r$, $\alpha_3 = z$. The cylindrical surface region is lubricated with the monotone generating line $\alpha_3 = z$ always inside the intervals: $0 < \varphi < \pi/2$; $-b/2 < z < +b/2$, z – longitudinal coordinate. Thus, the Lame coefficients are as follows: $h_1 = R$, $h_3 = 1$, where $R[m] = L_R$ denotes the radius of the cylindrical bone. Hence, we have: $U = \omega R$, $\Omega = \pi R b/2$.

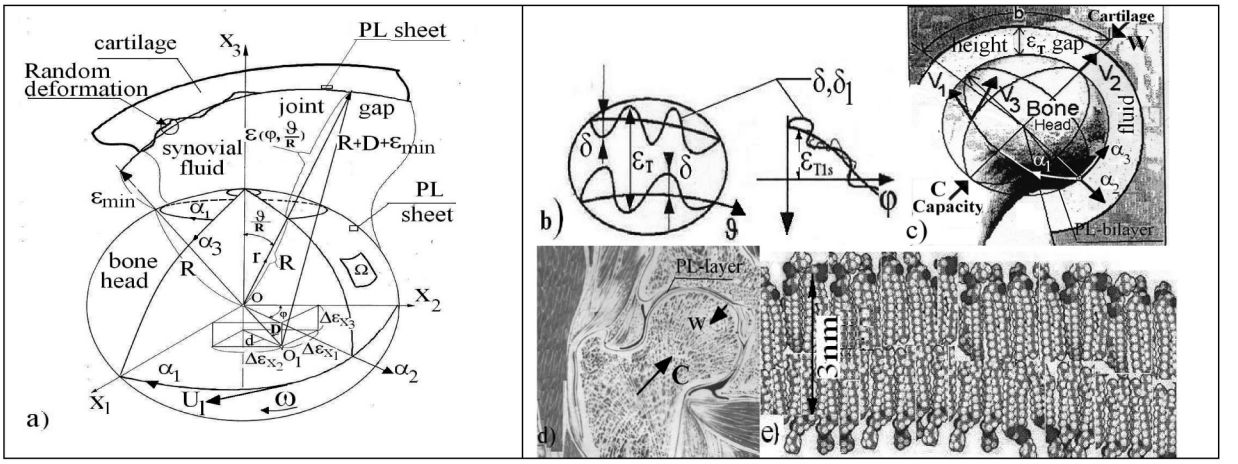

Fig. 4. Gap height between random deformable spherical cartilage surface: a) geometrical simulation of hip bone head and sleeve; b) random variation correction δ of the gap height ε_T; c) view of the hip joint gap; d) vertical section of the hip joint in the plane of anti-distortion angle; e) phospholipid (PL) bilayer (the height about 3 nm) on the internal sleeve and bonehead surface; R – radius of the bone head, ε_{min}– the least value of the gap height, C – capacity, W– load

Rys. 4. Wysokość szczeliny między odkształcalnymi losowo sferycznymi powierzchniami chrząstki: a) geometryczna symulacja głowy kostnej biodra i panewki; b) losowe zmiany korekt δ dla wysokości szczeliny ε_T; c) staw biodrowy; d) pionowy przekrój głowy stawu biodra; e) dwuwarstwa fosfolipidów (PL), o grubości 3 nm, na wewnętrznej powierzchni głowy biodra i panewki; R – promień głowy kostnej biodra, ε_{min} – najmniejsza wysokość szczeliny, C – nośność, W – obciążenie

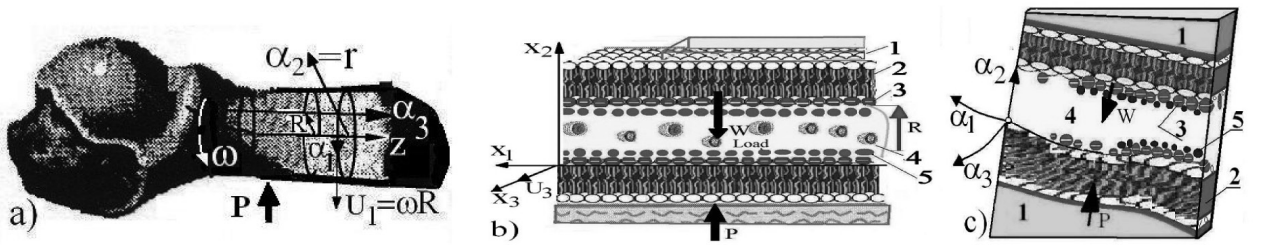

Fig. 5. Geometry of two cooperating surfaces: a) rotational region of cylindrical elbow joint; b) movable but non-rotational parallel planes; c) movable non – rotational and non – parallel surfaces; 1 – collagen region, 2 – PL – bilayer, 3 – hydrated phospholipid, 4 – synovial liquid, 5 – hydrated sodium ions, R – repulsion force, W – load, P – hydrodynamic pressure

Fig. 5. Geometria dwóch powierzchni: a) walcowy, obrotowy obszar stawu łokciowego, b) ruchome, nieobrotowe oraz równoległe płaszczyzny biologiczne, c) ruchome, nieobrotowe i nierównoległe powierzchnie; 1 – obszar kolagenu, 2 – PL – dwuwarstwa fosfolipidów, 3 – nawodniony fosfolipid, 4 – ciecz synowialna, 5 – nawodniony jon sodu, R – siła odpychająca, W – obciążenie, P – ciśnienie hydrodynamiczne

Example 3. Two non-rotational parallel plane surfaces are presented in **Fig. 5b**. As a particular case, we assume the thin biological liquid layer restricted by the two cooperating non-rotational but parallel biological planes in rectangular Cartesian coordinates $\alpha_1 = x_1$, $\alpha_2 = x_2$, and $\alpha_3 = x_3$. The Lame coefficients have the following form: $h_2 = 1$ and $h_1 = 1$, $h_3 = 1$ and $0 < x_1 < a$, $0 < x_3 < b \equiv L_R$ For example, this case is valid for ankle joints and in some regions occurring in the collar bone, the shoulder blade, and between the skin and tightly fitting clothing. Lower bone (or skin) surface moves in the $\alpha_3 = x_3$ direction with linear velocity U_3. The upper bone (or tightly fitting clothing) surface is motionless. Both parallel surfaces are motionless in the meridian $\alpha_1 = x_1$ direction, hence $U_1 = 0$ and $U = U_3$, $\Omega = ab$.

Example 4. This case valid for two movable, non-rotational and non-parallel surfaces presented in **Fig. 5c,** where $h_1 = h_1(\alpha_1,\alpha_3)$ and $h_3 = h_3(\alpha_1,\alpha_3)$.

RESULTS AFTER MEASUREMENTS AND NUMERICAL CALCULATIONS

We should have measured the real probability density function *f* of random gap height change for spherical hip joint (see Example1, **Figs. 4a, b, c,** and **d**), for cylindrical elbow gap height (see Example 2, **Fig. 5a**), and for two cooperating moving non-rotational biological planes occurring in ankle joint (see Example 3,4, **Figs. 5b** and **c)**. We should have considered the expected values *m* of gap height and standard deviation to obtain intervals of analytical bio-tribology parameters (26) – (29). Experimental measurement **[L. 1]** and **[L. 2]** of the mentioned joints gap height with radial clearance ε_0 from 2 to 10 μm should have proved that the dimensionless random variable of corrections for gap height, marked with the symbol δ_1, is most often manifested by two characteristic types of probability density functions. These are symmetrical and anti-symmetrical functions.

Symmetrical density functions f_s of correction parameters occur much less frequently than anti-symmetrical functions (about 12 times in 100 measurements with a probability of $P_s = 0.12$). They are characterized by a symmetrical distribution of random probability changes in terms of gap height increases and decreases.

The probabilities of random increases in joint height gap are equal to the probabilities of random decreases.

Among the frequently occurring unsymmetrical correction parameter, density functions describing random increases and decreases in gap height, we generally have two types of functions. The first type concerns function f_N, where the probabilities of random gap height increases dominate over the probabilities of random gap height decreases. The second type concerns function f_n, where the probabilities of random gap height decreases dominate over the probabilities of random gap height increases.

The two cases for anti-symmetrical probability density distribution functions, each one of them occur 22 times in 100 measurements with probability $P_N = 0.22$. The next two cases for anti-symmetrical probability density distribution functions f_n, each one of them occur 22 times in 100 measurements with probability $P_n = 0.22$. The measurement multiplicity (equal to 12+2×22+2×22 = 100) creates a probabilistic complete system of events.

Based on the obtained abovementioned probability density functions f_s, f_N, f_n of random changes, we should have determined the average expected value and standard deviation of gap height for: spherical hip (m_h,σ_h) cylindrical elbow (m_e,σ_e) and plane ankle (m_j,σ_j) surfaces. If we put these values into the inequalities above (26)-(29), then we obtain the following upper and lower estimation of fractions: $\xi_p^h, \xi_C^h, \xi_F^h, \xi_\mu^h; \xi_p^e, \xi_C^e, \xi_F^e, \xi_\mu^e; \xi_p^j, \xi_C^j, \xi_F^j, \xi_\mu^j$ for hip, elbow, and ankle cooperating joint surfaces with upper index *h ,e, j* respectively:

$$0.3177\cdot\alpha_p^h \le \left(\xi_p^h \equiv \frac{EX(p)}{p(\delta_1=0)}\right) \le 3.7055\cdot\beta_p^h, \quad 0.3177\cdot\alpha_C^h \le \left(\xi_C^h \equiv \frac{EX(C)}{C(\delta_1=0)}\right) \le 3.7055\cdot\beta_C^h,$$
$$0.4409\cdot\alpha_F^h \le \left(\xi_F^h \equiv \frac{EX(F_R)}{F_R(\delta_1=0)}\right) \le 2.2678\cdot\beta_F^h, \quad 0.6120\cdot\alpha_\mu^h \le \left(\xi_\mu^h \equiv \frac{EX(\mu)}{\mu(\delta_1=0)}\right) \le 1.3879\cdot\beta_\mu^h, \tag{31a}$$

$$0.3277\times\alpha_p^e \le \left(\xi_p^e \equiv \frac{EX(p)}{p(\delta_1=0)}\right) \le 3.6055\cdot\beta_p^e, \quad 0.3277\cdot\alpha_C^e \le \left(\xi_C^e \equiv \frac{EX(C)}{C(\delta_1=0)}\right) \le 3.6055\cdot\beta_C^e,$$
$$0.4509\cdot\alpha_F^e \le \left(\xi_F^e \equiv \frac{EX(F_R)}{F_R(\delta_1=0)}\right) \le 2.1678\cdot\beta_F^e, \quad 0.6220\cdot\alpha_\mu^e \le \left(\xi_\mu^e \equiv \frac{EX(\mu)}{\mu(\delta_1=0)}\right) \le 1.2879\cdot\beta_\mu^e, \tag{31b}$$

$$0.3377\cdot\alpha_p^j \le \left(\xi_p^j \equiv \frac{EX(p)}{p(\delta_1=0)}\right) \le 3.505\cdot\beta_p^j, \quad 0.3377\cdot\alpha_C^j \le \left(\xi_C^j \equiv \frac{EX(C)}{C(\delta_1=0)}\right) \le 3.5055\cdot\beta_C^j,$$
$$0.4609\cdot\alpha_F^j \le \left(\xi_F^j \equiv \frac{EX(F_R)}{F_R(\delta_1=0)}\right) \le 2.0678\cdot\beta_F^j, \quad 0.6320\cdot\alpha_\mu^j \le \left(\xi_\mu^j \equiv \frac{EX(\mu)}{\mu(\delta_1=0)}\right) \le 1.1879\cdot\beta_\mu^j. \tag{31c}$$

The upper and lower estimation values of dimensionless fractions (quotients) ξ_p, ξ_C, ξ_F, ξ_μ of pressure, capacity, friction forces, friction coefficients presented in Equations (31a, b, and c) with upper indexes: *h,e,j,* require to find corrections coefficients α_p, α_C, α_F, α_μ, β_p, β_C, β_F, β_μ each with upper indexes *h, e, j*. Therefore, now we are going to determine the numerical solutions of stochastic partial differential Equations (4) to (9) for spherical hip, cylindrical elbow, and ankle joints. The sketch of the numerical solutions of the system of (4)–(9) and its half-analytical solutions and integrals (16)–(17) mainly concern stochastic and non-stochastic (excluding operator *EX*) non-linear partial differential equation for spherical hip, cylindrical elbow, and ankle joints. The denominators of fractions: $\xi^h_p, \xi^h_C, \xi^h_F, \xi^h_\mu; \xi^e_p, \xi^e_C, \xi^e_F, \xi^e_\mu; \xi^j_p, \xi^j_C, \xi^j_F, \xi^j_\mu$ defined in Equations (31a, b, and c) are the numerical solutions from the system of Equations (4) to (9) excluding the random operator *EX* by assuming a gap height without stochastic decrease or increase. The fraction nominators are presented in the numerical solutions of the system (4)–(9) assuming stochastic changes of gap height. The abovementioned fractions ξ with upper index *h,e, j* are dependent on radial clearances (characteristic values of gap height ε_0) and the dimensionless range of stochastic changes of solutions of Equations (4) to (9) represented random expected values of gap height for the concretely numerical elaborated calculations of hip, elbow, and ankle joints. The dimensionless estimations of fractions ξ_p, ξ_C, ξ_F, ξ_μ with upper indexes *h, e, j* for human hip, elbow, and ankle joint lubrication parameters, presented in Equations (31a, b, and c), as quotients obtained after numerical solutions of Equations (4) to (9) have finally the lower and upper estimation in the following form:

$$\xi^h_{p\,min} \le \xi^h_p \le \xi^h_{p\,max}, \quad \xi^h_{C\,min} \le \xi^h_C \le \xi^h_{C\,max}, \quad \xi^h_{F\,min} \le \xi^h_F \le \xi^h_{F\,max}, \quad \xi^h_{\mu\,min} \le \xi^h_\mu \le \xi^h_{\mu\,max}, \tag{32a}$$

$$\xi^e_{p\,min} \le \xi^e_p \le \xi^e_{p\,max}, \quad \xi^e_{C\,min} \le \xi^e_C \le \xi^e_{C\,max}, \quad \xi^e_{F\,min} \le \xi^e_F \le \xi^e_{F\,max}, \quad \xi^e_{\mu\,min} \le \xi^e_\mu \le \xi^e_{\mu\,max}, \tag{32b}$$

$$\xi^j_{p\,min} \le \xi^j_p \le \xi^j_{p\,max}, \quad \xi^j_{C\,min} \le \xi^j_C \le \xi^j_{C\,max}, \quad \xi^j_{F\,min} \le \xi^j_F \le \xi^j_{F\,max}, \quad \xi^j_{\mu\,min} \le \xi^j_\mu \le \xi^j_{\mu\,max}. \tag{32c}$$

We calculate fraction ξ_{min} by assuming the stochastic changes of lubrication parameters for which the fraction value is the lowest. We calculate fraction nominators ξ_{max} by assuming the stochastic changes for which the fraction value is the highest. After numerical calculations, the maximum and minimum extreme values ξ_{max}, ξ_{min} for spherical hip joints only were obtained and presented in **Tab. 1** as quotients (26–29) of stochastic values to non-stochastic values for pressure, load carrying capacity, friction forces, coefficients of friction.

Table 1. Extreme numerical values ξ^h_{max}, ξ^h_{min}, describing ratio of solution (pressure *p*, capacity *C*, friction forces *F*, friction coefficient μ) obtained from the system of Equations (4) to (9) for stochastic changes in the hip joint gap height with radial clearance 2 μm $\le \varepsilon_0 \le$ 10 μm, to the same solutions by assuming a gap height without random changes

Tabela 1. Ekstremalne wartości numeryczne ξ^h_{max}, ξ^h_{min}, będące stosunkiem rozwiązań (ciśnienia *p*, nośności *C*, sił tarcia *F*, współczynnika tarcia μ wyznaczonego z układu równań (4–9) dla losowych zmian wysokości szczeliny stawu biodra o luzach ε_0 w przedziale [2 μm, 10 μm], do tych samych rozwiązań w przypadku wysokości szczeliny bez losowych zmian

ξ^h \ ε_0	2 μm	4 μm	6 μm	8 μm	10 μm
$\xi_{p\,min}$	0.558664	0.560021	0.561597	0.563306	0.566334
$\xi_{p\,max}$	2.387635	2.372290	2.352564	2.314966	2.259481
$\xi_{C\,min}$	0.557866	0.558636	0.559780	0.561197	0.563589
$\xi_{C\,max}$	2.393302	2.383636	2.367265	2.331374	2.272007
$\xi_{F\,min}$	0.824445	0.879285	0.897883	0.905707	0.909492
$\xi_{F\,max}$	1.267801	1.113264	1.089166	1.077987	1.071942
$\xi_{\mu\,min}$	0.344412	0.369016	0.379336	0.388493	0.400410
$\xi_{\mu\,max}$	2.272391	1.992623	1.945346	1.920080	1.902154

CONCLUSIONS FOR MOVABLE NON ROTATIONAL BIO-SURFACES

1. This work presents an analytical, non-isothermal, stochastic, laminar model of the hydrodynamic theory of lubrication of human joint-nodes, taking into account the phospholipid layer, covering the non-rotational cooperating arbitrary bio-surfaces. Here are assumed random changes not only in gap height, but also random changes of viscosity and velocity of non-Newtonian synovial fluid. Moreover, the influences of these changes on the expected values of bio-tribology parameters, such as pressure, load-carrying capacity, frictional force, and coefficient of friction, were determined in Equations (26) to (29) for various shapes of non-rotational and rotational cooperating biological surfaces.
2. Based on the stochastic equations of hydrodynamic lubrication theory of non-rotational surfaces and their semi-analytical-numerical solutions, upper and lower estimations of the expected values of joint gap height, synovial fluid (SF) flow velocity (24), and apparent viscosity (25) of SF were determined. These estimations are functions of standard deviation σ and the expected values m of gap height obtained from values of probability density functions f of gap height determined in an experimental way. Finally, the general estimations were determined for the expected value of pressure (26), joint-carrying capacity (27), frictional force (28), and coefficient of friction (29) for various shapes of cooperating bio-surfaces.
3. The presented model of hydrodynamic joint lubrication theory takes into account changes in the viscosity of synovial fluid in the direction of the gap height and the influence of the superficial layer properties of the flowed around curvilinear articular cartilage surface on the viscosity of synovial fluid.
4. The general random solutions (9), (16a, b), for biological fluid viscosity $EX(\eta T)$ and velocity $EX(v)$ obtained for arbitrary non-rotational cooperating biological surfaces imply the stochastic estimations, (25) and (24), showing the decrease and increase in the value of biological fluid viscosity ηT and fluid flow velocity v in the biological friction gap between non-rotational surfaces, compared to the viscosity and velocity obtained without taking into account random changes in gap height for $\delta_1 = 0$. The decrease and increase are dependent on expected values m of gap height and its standard deviations σ.

REFERENCES

1. Cwanek J.: The usability of the surface geometry parameters for the evaluation of the artificial hip joint wear. Rzeszów University Press, Rzeszów 2009.
2. Mow VC., Ratcliffe A., Woo S.: Biomechanics of Diarthrodial Joints. Springer Verlag, Berlin, N. Y. 1990.
3. Wierzcholski K.: Time depended human hip joint lubrication for periodic motion with stochastic asymmetric density function. Acta of Bioengineering and Biomechanics, 2014, 16 (1), pp. 83–97.
4. Andersen O.S., Roger E. et. al.: Bilayer thickness and Membrane Protein Function: An Energetic Perspective. Annular Review of Biophysics and Biomolecular Structure, 2014, 36 (1), pp. 107–130.
5. Bhushan B.: Nanotribology and nanomechanics of MEMS/NEMS and BioMEMS/BioNEMS materials and devices. Microelectronic Engineering, 2007, 84, pp. 387–412.
6. Bhushan B.: Handbook of Micro/Nano Tribology, second ed. CRC Press. Boca Raton, London, New York, Washington D.C. 1999.
7. Chagnon G., Rebouah M., Favier D.: Hyperelastic Energy Densities for Soft Biological Tissues, A Review. Journal of Elasticity, 2015, 120 (2), pp. 129–160.
8. Gadomski A., Bełdowski P., Miguel Rubi J., Urbaniak W., Wayne K., Auge W.K., Holek I.S., Pawlak Z.: Some conceptual thoughts toward nano–scale oriented friction in a model of articular cartilage. Mathematical Biosciences, 2013, 244, pp. 188–200.
9. Hills B.A.: Oligolamellar lubrication of joint by surface active phospholipid. J. of Reumatology, 1989, 16, pp. 82–91.
10. Hills B.A.: Boundary lubrication in vivo. Proc. Inst. Mech. Eng. Part H: J. Eng. Med., 2000, 214, pp. 83–87.
11. Marra J., Israelachvili J.N.: Direct measurements of forces between phosphatidylcholine and phosphatidylethanolamine bilayers in aqueous electrolyte solutions, Biochemistry, 1985, 24, pp. 4608–4618.
12. Schwarz I.M., Hills B.A.: Synovial surfactant: Lamellar bodies in type B synoviocytes and proteolipid in synovial fluid and the articular lining. British Journal of Rheumatology, 1966, 35 (9), pp. 821–827.

13. Pawlak Z., Figaszewski Z.A., Gadomski A., Urbaniak W., Oloyede A.: The ultra-low friction of the articular surface is pH-dependent and is built on a hydrophobic underlay including a hypothesis on joint lubrication mechanism. Tribology International, 2010, 43, pp. 1719–1725.
14. Pawlak Z., Urbaniak W., Oloyede A.: The relationship between friction and wettability in aqueous environment of natural joints, Wear, 2011, 271, pp. 1745–1749.
15. Pawlak Z., Urbaniak W., Gadomski A., Kehinde Q., Fusuf K.Q., Afara I.O., Oloyede A.: The role of lamellate phospholipid bilayers in lubrication of joints. Acta of Bioeng.and Biomech., 2012, 14 (4), pp. 101–106.
16. Pawlak Z., Urbaniak W., Hagner-Derengowska M.W.: The Probable Explanation for the Low Friction of Natural Joints, Cell Biochemistry and Biophysics, 2015, 71 (3), pp. 1615–1621.
17. Pawlak Z., Gadomski A., Sojka M., Urbaniak W., Bełdowski P.: The amphoteric effect on friction between the bovine cartilage/cartilage surfaces under slightly sheared hydration lubrication model,.Colloidsand Surfaces B: Biointerfaces, Octo. 1, 146:452–8, doi: 10.1016/j.colsurfb., 2016,06.027.
18. Petelska A.D., Figaszewski Z.A.: Effect of pH on interfacial tension of bilayer lipid membrane. Biophysical Journal, 2000, 78, pp. 812–817.
19. Wierzcholski K., Miszczak A.: Electro-Magneto-Hydrodynamic Lubrication. Open Physics, 2018, 16 (1), pp. 285–291.
20. Wierzcholski K., Miszczak A.: Mathematical principles and methods of biological surface lubrication with phospholipids bilayers,www.elsevier.com. Biosystems, 2019, 178 (2019), pp. 32–40.
21. Wierzcholski K.: Topology of calculating pressure and friction coefficients for time-dependent human hip joint lubrication. Acta of Bioengineering and Biomechanics, 2011, 13 (1), pp. 41–56.
22. Wierzcholski K.: Joint cartilage lubrication with phospholipids bilayer. Tribologia, 2016, 2 (265), pp. 145–157.
23. Wierzcholski K.: Determination of the random friction forces on the biological surfaces of human hip joint with phospholipid bilayer. Tribologia, 2019, 2, pp. 131–142.
24. Helwig Z.: Elements of probability calculations and mathematical statistics, in Polish: Elementy rachunku prawdopodobieństwa i statystyki matematycznej. PWN, Warszawa 1977.
25. Fisz M.: Probabilisty calculation and mathematical statistics, in Polish: Rachunek prawdopodobińśtwa i statystyka matematyczna. PWN, Warszawa 1967.
26. Yuan C.Q., Peng Z., Yan X.P., Zhou X.C.: Surface roughness evaluation in sliding wear process. Wear, 2008, 265, pp. 341–348.
27. Syrek P.: Analiza parametrów przestrzennych aplikatorów małogabarytowych, wykorzystywanych w magnetoterapii. AGH University of Sciences and Technology, Kraków, doctor thesis, 2010.